2010 IEEE International Conference on Robotics and Automation
Anchorage Convention District
May 3-8, 2010, Anchorage, Alaska, USA

Sensorless Linear Induction Motor Control using Fuzzy Observers for Speed Tracking

Peter Liu, *Member, IEEE*, Cheng-Yao Hung, Chian-Song Chiu and Kuang-Yow Lian, *Member, IEEE*

***Abstract*— In this paper, a sensorless speed controller for linear induction motor (LIM) is developed based on a fuzzy observer. First, the LIM is represented by a T-S fuzzy model. Next, the fuzzy observer is constructed to estimate the immeasurable states including the mover speed and secondary flux, where the observer gains are obtained by computationally solving a set of linear matrix inequalities. Based on the fuzzy observer, the synthesis using the virtual desired variable concept is applied to design the control law. Then, the exponential convergence for both estimation error and tracking error is concluded. This indicates that the proposed sensorless speed control possesses the feature with fast transient response and high robustness. Finally, experiments are carried out to verify the theoretical results and show satisfactory performance.**

I. Introduction

The linear induction motor (LIM) has performance features such as high starting thrust force, alleviation of gear between motor and the motion devices, and reduced mechanical losses, etc [1]-[5]. From the aforementioned advantages, industrial applications widely adopt LIMs, including transportation systems, conveyor systems, actuators, and material handling, which achieve satisfactory performance. The requirement of speed transducers, such as a linear encoder or resolver, is necessary for the feedback systems to achieve motion control. However, this increases not only the cost, weight, and complexity but also degrades the robustness and reliability of the system. To avoid the mainly mechanical based sensors, sensorless control strategies have been adopted. Several research results have been done to eliminate the sensors [6], [7].

Takagi-Sugeno (T-S) fuzzy model [8] have been extensively used the represent nonlinear systems using fuzzy rules which then utilize conventional linear control methods. Controller and observer gains may be computationally solved from stability criteria formulated into linear matrix inequalities (Here, we do not abbreviate linear matrix inequalities into LMI for clarity). In this paper, we propose a novel speed sensorless control for the full fifth-order model of LIMs based on the fuzzy observer design to estimate the immeasurable variables including mover speed and secondary flux. By membership functions fitting a Lipschitz-like property, it can be proven that estimation errors converge to zero exponentially. After the fuzzy observer has been designed, the speed tracking controller is separately developed based on the VDV (virtual desired variable), i.e., the estimated states are used to replace the real states. In details, we first formulate the speed tracking control into a force tracking problem [9]. Then, a set of VDVs including virtual desired current and fluxes are introduced to synthesize the controller. In the design, a skew-symmetric property pertaining to the dynamics of the LIM is utilized to simplify the structure of the controller. Using this controller, the tracking error converges to zero exponentially. The feature of exponential convergence for both the estimation and tracking errors shows the fast transient response and high robustness. To demonstrate the effectiveness of the proposed scheme, a voltage-fed drive system is used as an example to achieve speed tracking. For uncertain loads or large parametric uncertainties, the experimental results still maintain good performance.

The rest of the paper is organized as follows. In Section II, describes the LIM mathematical model in the *a-b* stationary reference frame. Then, the LIM furthermore transformed in T-S fuzzy model form is presented in Section III. In Section IV, the T-S fuzzy observer design is presented. The design method of the overall controller is synthesized in Section V. In Section VI, the experimental results are given to show the control performance. Finally, some conclusions are made in Section VII.

II. Dynamical Model of LIMs

The fifth-order dynamic model of the LIM in *a-b* stationary reference frame is described by [10]-[12]:

$$\begin{aligned}
\dot{i}_{pa} &= -\tfrac{\gamma}{\sigma} i_{pa} + \tfrac{\pi n_p}{\sigma \ell} v_m \lambda_{sb} + \tfrac{R_s}{\sigma L_s} \lambda_{sa} + \tfrac{L_s}{\sigma L_m} V_{pa} \\
\dot{i}_{pb} &= -\tfrac{\gamma}{\sigma} i_{pb} - \tfrac{\pi n_p}{\sigma \ell} v_m \lambda_{sa} + \tfrac{R_s}{\sigma L_s} \lambda_{sb} + \tfrac{L_s}{\sigma L_m} V_{pb} \\
\dot{\lambda}_{sa} &= \tfrac{L_m R_s}{L_s} i_{pa} - \tfrac{\pi n_p}{\ell} v_m \lambda_{sb} - \tfrac{R_s}{L_s} \lambda_{sa} \\
\dot{\lambda}_{sb} &= \tfrac{L_m R_s}{L_s} i_{pb} + \tfrac{\pi n_p}{\ell} v_m \lambda_{sa} - \tfrac{R_s}{L_s} \lambda_{sb} \\
\dot{v}_m &= \tfrac{F}{M} - \tfrac{F_l}{M} - \tfrac{D}{M} v_m
\end{aligned} \tag{1}$$

where $\gamma = \left(\frac{L_s R_p}{L_m} + \frac{L_m R_s}{L_s} \right)$, $\sigma = L_s L_p / L_m - L_m$, $F = \kappa \left(i_{pb} \lambda_{sa} - i_{pa} \lambda_{sb} \right)$, $\kappa = 3\pi n_p L_m / 2\ell L_s$, and

Peter Liu is an Assistant Professor with Dept. of Electrical Engineering, Tamkang University, Tamsui, Taipei County, Taiwan (Corresponding author: phone: +886-2-2621-5656 ext. 2582; fax: +886-2-2620-9814; email: pliu@ieee.org)

C.-Y Hung is with the System Development, Display BU, Wistron Corporation, Taipei allen_cy_hung@wistron.com

C.-S Chiu is a Associate Professor with the Dept. of Electrical Engineering, Chung-Yuan Christian University, Chung-Li, Taiwan cschiu@dec.ee.cycu.edu.tw

K.-Y Lian is a Professor with the Dept. of Electrical Engineering, National Taipei University of Technology, Taipei, Taiwan kylian@ntut.edu.tw

i_{pa} (i_{pb})	a-axis and b-axis primary current;
V_{pa} (V_{pb})	a-axis and b-axis primary voltage;
λ_{sa} (λ_{sb})	a-axis and b-axis secondary flux;
R_p (R_s)	primary (secondary) resistance;
L_p (L_s)	primary (secondary) inductance;
$v_m L_m$	mover speed, mutual inductance;
ℓ, M	pole pitch, primary mass;
D, n_p	viscous friction, number of pole pairs;
F_l, κ	load disturbance, force constant;
F	electromechanical coupling force;

The longitudinal end-effect is approximated by Taylor's series and can be taken as an external load force $F_l = \theta_1 + \theta_2 v_m + \theta_3 v_m^2$. This end-effect increases with the speed of the primary [13], [14]. The nominal part of the load force can be included in the damping force, and the remainder is formulated as an amount of uncertainty in the system. A rigorous design to deal with the uncertainty using adaptive technique will lead to the mixed problem of simultaneously identifying the parameters and estimating state variables. This will yield complex control law. An alternative is to cope with this small amount of uncertainty by a high robust controller. The controller to be proposed will make the error system exponentially stable and is very robust to uncertainty.

The dynamical model possess a skew-symmetric property in its state equations for unmeasurable variables, which will be used in controller design. To see this, we rearrange the dynamical equations by using more compact notations. Denote $\underline{x} = [x_1,\, x_2,\, x_3,\, x_4]^\top = [i_{pa},\, i_{pb},\, \lambda_{sa},\, \lambda_{sb}]^\top$. The model (1) can be rewritten as

$$Q\dot{\underline{x}} + G(v_m)\,\underline{x} + R(v_m)\,\underline{x} = \upsilon \tag{2}$$

$$M\dot{v}_m + Dv_m = F - F_l \tag{3}$$

where $\upsilon = \left[\frac{L_s}{L_m}V_{pa},\, \frac{L_s}{L_m}V_{pb},\, 0,\, 0\right]^\top$, $\gamma = \left(\frac{L_s R_p}{L_m} + \frac{L_m R_s}{L_s}\right)$ and

$$Q = \begin{bmatrix} \sigma\mathbf{I}_2 & 0 \\ 0 & \mathbf{I}_2 \end{bmatrix},\ G(v_m) = \begin{bmatrix} 0 & 0 \\ 0 & -\mathbf{J}_2 \end{bmatrix}\frac{\pi n_p}{\ell}v_m,$$

$$\mathbf{I}_2 = \begin{bmatrix} 1 & 0 \\ 0 & 1 \end{bmatrix},\ \mathbf{J}_2 = \begin{bmatrix} 0 & -1 \\ 1 & 0 \end{bmatrix},$$

$$R(v_m) = \begin{bmatrix} \gamma\mathbf{I}_2 & \frac{\pi n_p}{\ell}v_m\mathbf{J}_2 - \frac{R_s}{L_s}\mathbf{I}_2 \\ -\frac{L_m R_s}{L_s}\mathbf{I}_2 & \frac{R_s}{L_s}\mathbf{I}_2 \end{bmatrix},$$

The LIM dynamical model possesses a skew-symmetric property in its state equations for measurable variables, which will be used in our controller design. The term $G(v_m)$ is a skew-symmetric matrix. The skew-symmetric matrix represents a "workless force" in the physical sense, which does not affect the energy balance and system stability. Thus, $G(v_m)$ is not needed to be canceled in the control law to be simplified in Section V.

III. T-S Fuzzy Representation

The T-S fuzzy dynamic models described by fuzzy IF-THEN rules are utilized to exactly represent the LIM in a region of interest. To express the LIM in terms of a T-S fuzzy model, we further rewrite Eqs. (2)∼(3) in the following form:

$$\begin{aligned} \dot{x}(t) &= A(x)\,x(t) + Bu + bF_l \\ y(t) &= Cx(t) \end{aligned} \tag{4}$$

where $x(t) = \begin{bmatrix} x_1 & x_2 & x_3 & x_4 & x_5 \end{bmatrix}^\top = \begin{bmatrix} i_{pa} & i_{pb} & \lambda_{sa} & \lambda_{sb} & v_m \end{bmatrix}^\top$ are the overall states; $y(t) = \begin{bmatrix} i_{pa} & i_{pb} \end{bmatrix}^\top$ are the measurable output; $u = \begin{bmatrix} V_{pa} & V_{pb} \end{bmatrix}^\top = \begin{bmatrix} u_1 & u_2 \end{bmatrix}^\top$ are the control input; F_l are the known external load; and the associated matrices and vector:

$$A(x) = \begin{bmatrix} -\frac{\gamma}{\sigma} & 0 & \frac{R_s}{\sigma L_s} & 0 & \frac{\pi n_p}{\sigma\ell}\lambda_{sb} \\ 0 & -\frac{\gamma}{\sigma} & 0 & \frac{R_s}{\sigma L_s} & -\frac{\pi n_p}{\sigma\ell}\lambda_{sa} \\ \frac{L_m R_s}{L_s} & 0 & -\frac{R_s}{L_s} & -\frac{\pi n_p}{\ell}v_m & 0 \\ 0 & \frac{L_m R_s}{L_s} & \frac{\pi n_p}{\ell}v_m & -\frac{R_s}{L_s} & 0 \\ -\frac{\kappa}{M}\lambda_{sb} & \frac{\kappa}{M}\lambda_{sa} & 0 & 0 & -\frac{D}{M} \end{bmatrix},$$

$$B = \begin{bmatrix} \frac{L_s}{\sigma L_m} & 0 \\ 0 & \frac{L_s}{\sigma L_m} \\ 0 & 0 \\ 0 & 0 \\ 0 & 0 \end{bmatrix},\ b = \begin{bmatrix} 0 \\ 0 \\ 0 \\ 0 \\ -\frac{1}{M} \end{bmatrix},\ C = \begin{bmatrix} 1 & 0 \\ 0 & 1 \\ 0 & 0 \\ 0 & 0 \\ 0 & 0 \end{bmatrix}^\top.$$

Then, according to [15], the T-S fuzzy model representation of (4) can be expressed by the following rules:

Plant Rule i :

IF λ_{sa} is F_{1i} and λ_{sb} is F_{2i} and v_m is F_{3i} THEN

$$\begin{aligned} \dot{x}(t) &= A_i x(t) + Bu(t) + bF_l \\ y(t) &= Cx(t),\ i = 1, \cdots, 8 \end{aligned} \tag{5}$$

where λ_{sa}, λ_{sb}, and v_m are premise variables which are immeasurable. The fuzzy sets $F_{ji} (j = 1,\, 2,\, 3)$ are set to $F_{11} = F_{12} = F_{13} = F_{14} = \frac{x_3 - d_1}{D_1 - d_1}$; $F_{15} = F_{16} = F_{17} = F_{18} = \frac{D_1 - x_3}{D_1 - d_1}$; $F_{21} = F_{22} = F_{25} = F_{26} = \frac{x_4 - d_2}{D_2 - d_2}$; $F_{23} = F_{24} = F_{27} = F_{28} = \frac{D_2 - x_4}{D_2 - d_2}$; and $F_{31} = F_{33} = F_{35} = F_{37} = \frac{x_5 - d_3}{D_3 - d_3}$; $F_{32} = F_{34} = F_{36} = F_{38} = \frac{D_3 - x_5}{D_3 - d_3}$. The system matrices A_i of subsystem i are given by

$$A_i = \begin{bmatrix} -\frac{\gamma}{\sigma} & 0 & \frac{R_s}{\sigma L_s} & 0 & \frac{\pi n_p}{\sigma\ell}\delta_i \\ 0 & -\frac{\gamma}{\sigma} & 0 & \frac{R_s}{\sigma L_s} & -\frac{\pi n_p}{\sigma\ell}\varphi_i \\ \frac{L_m R_s}{L_s} & 0 & -\frac{R_s}{L_s} & -\frac{\pi n_p}{\ell}\vartheta_i & 0 \\ 0 & \frac{L_m R_s}{L_s} & \frac{\pi n_p}{\ell}\vartheta_i & -\frac{R_s}{L_s} & 0 \\ -\frac{\kappa}{M}\delta_i & \frac{\kappa}{M}\varphi_i & 0 & 0 & -\frac{D}{M} \end{bmatrix}$$

where $\varphi_1 = D_1$, $\delta_1 = D_2$, $\vartheta_1 = D_3$; $\varphi_2 = D_1$, $\delta_2 = D_2$, $\vartheta_2 = d_3$;$\varphi_3 = D_1$, $\delta_3 = d_2$, $\vartheta_3 = D_3$; $\varphi_4 = D_1$, $\delta_4 = d_2$, $\vartheta_4 = d_3$; $\varphi_5 = d_1$, $\delta_5 = D_2$, $\vartheta_5 = D_3$; $\varphi_6 = d_1$, $\delta_6 = D_2$, $\vartheta_6 = d_3$; and $\varphi_7 = d_1$, $\delta_7 = d_2$, $\vartheta_7 = D_3$; $\varphi_8 = d_1$, $\delta_8 = d_2$, $\vartheta_8 = d_3$. In these fuzzy rules, D_1 and d_1 are the upper bound and lower bound of λ_{sa}, respectively; D_2, d_2 are the upper bound and lower bounded of λ_{sb}, respectively; D_3 and

d_3 are the upper bound and lower bound of v_m, respectively. Using the singleton fuzzifier, product fuzzy inference and weighted average defuzzifier, the final output of the fuzzy system is inferred as follows:

$$\dot{x}(t) = \sum_{i=1}^{8} \mu_i(x(t)) \{A_i x(t) + Bu(t) + bF_l\}$$
$$y(t) = Cx(t), \tag{6}$$

where $\mu_i(x(t)) = \phi_i(x(t)) / \sum_{i=1}^{8} \phi_i(x(t))$ with $\phi_i(x(t)) = \prod_{j=1}^{3} F_{ji}(x(t))$. Note that $\sum_{i=1}^{8} \mu_i(x(t)) = 1$ for all t, where $\mu_i(x(t)) \geq 0$ for all $i = 1, \cdots, 8$. Based on the setting of F_{ji} and A_i, it can be checked that the inferred output is exactly equivalent to the model of the LIM (4).

Notice that the membership functions $F_{ij}(\cdot)$ satisfy $F_{ij}(x(t)) - F_{ij}(\widehat{x}(t)) = \eta_{ij}^{\top}(x(t) - \widehat{x}(t))$ for some bounded function vector $\eta_{ij}^{\top}$ and any x, $\widehat{x}$ in the universe of discourse. We can conclude the following property:

Property 1: *The grade function error is proportional to the estimation error $e = x - \hat{x}$, i.e., $\mu_i(x(t)) - \mu_i(\widehat{x}(t)) = \Lambda_i^{\top} e$ for some bounded function vector $\Lambda_i^{\top}$.*

IV. Fuzzy Observer Design

Now, we design the fuzzy observer to estimate the immeasurable states. The fuzzy observer is given as follows:

Observer Rule i :

IF $\hat{\lambda}_{sa}$ is F_{1i} and $\hat{\lambda}_{sb}$ is F_{2i} and $\hat{v}_m$ is F_{3i} THEN

$$\dot{\hat{x}}(t) = A_i \hat{x}(t) + Bu(t) + bF_l + L_i(y(t) - \hat{y}(t))$$
$$\hat{y}(t) = C\hat{x}(t), \ i = 1, \cdots, 8$$

where the premise variables $\hat{\lambda}_{sa}$, $\hat{\lambda}_{sb}$, and $\hat{v}_m$ are accordingly the estimations of λ_{sa}, λ_{sb}, and v_m, respectively; $\hat{x}(t)$ and $\hat{y}(t)$ denote the estimation of $x(t)$ and $y(t)$, respectively; and L_i is an observer gain to be determined later. The inferred output of the observer is

$$\dot{\hat{x}}(t) = \sum_{i=1}^{8} \mu_i(\widehat{x}(t)) \{A_i \hat{x}(t) + Bu(t) + bF_l + L_i(y(t) - \hat{y}(t))\}$$
$$\hat{y}(t) = C\hat{x}(t). \tag{7}$$

Define the state estimation error $e(t) = x(t) - \hat{x}(t)$. Subtracting (6) by (7), we have

$$\dot{e}(t) = \sum_{i=1}^{8} \mu_i(\widehat{x}(t)) \{(A_i - L_i C) e\} + h(t) \tag{8}$$

where $h(t) = \sum_{i=1}^{8} (\mu_i(x) - \mu_i(\widehat{x})) \{A_i x(t)\}$. The term $h(t)$ in (8) is unknown due to immeasurable premise variables λ_{sa}, λ_{sb}, and v_m. However, a closer investigation reveals a property for $h(t)$ addressed below.

In light of Property 1, we have $h(t) = \left(\sum_{i=1}^{8} A_i x(t) \Lambda_i^{\top}\right) e$. Supposed that $x(t)$ is bounded (this is confirmed in controller design), the term $h(t)$ satisfies the bound

$$h^{\top} h \leq e^{\top} U^{\top} U e \tag{9}$$

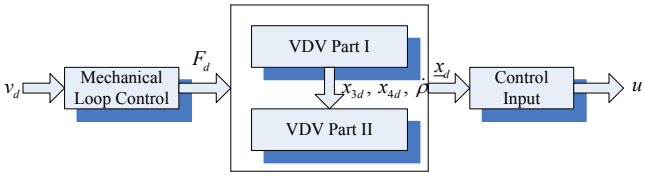

Fig. 1: The VDV design procedure.

with a symmetric positive-definite matrix U depending on $\Lambda_i^{\top}$ and x. Although the undesired term $h(t)$ will affect the estimation performance, suitably choosing observer gains L_i can attenuate $h(t)$ to zero exponentially. Now, we apply Lyapunov method to get the observer gains L_i.

Let us choose the Lyapunov function candidate $V_o(e(t)) = e^{\top}(t) P e(t)$. Taking the time derivative of V_o, we have $\dot{V}_o(e) = \sum_{i=1}^{8} \mu_i(\widehat{x}) e^{\top} \left[(A_i - L_i C)^{\top} P + P(A_i - L_i C)\right] e + h^{\top} P e + e^{\top} P h$.From (9) and $h^{\top} P e \leq \frac{1}{2} h^{\top} h + \frac{1}{2} e^{\top} P P e$, it follows that $h^{\top} P e + e^{\top} P h \leq e^{\top} \left(U^{\top} U + P P\right) e$.Therefore, the inequality for $\dot{V}_o(e)$ can be expressed as follows:

$$\dot{V}_o(e) \leq \sum_{i=1}^{8} \mu_i(\widehat{x}) e^{\top} G_i e - e^{\top} E P E e \tag{10}$$

where $G_i = A_i^{\top} P + P A_i - C^{\top} Z_i^{\top} - Z_i C + U^{\top} U + P P + E P E$. The symmetric positive-definite matrix E is introduced to dominate the estimation convergence rate. The first term in (10) is negative definite if the following linear matrix inequalities for $P > 0$ and Z_i is held.

$$\begin{bmatrix} A_i^{\top} P + P A_i - C^{\top} Z_i^{\top} - Z_i C + U^{\top} U + E P E & P \\ P & -I \end{bmatrix} < 0, \ \forall \ i = 1, \cdots, 8, \tag{11}$$

where $Z_i = P L_i$. Then, (10) is shown to be negative definite as $\dot{V}_o(e) \leq -e^{\top} E P E e$ which implies that $\widehat{x}(t)$ converges to $x(t)$ exponentially once $x(t)$ is conform to the discuss region.

Theorem 1: *For the fuzzy observer (7), suppose that all states and control input are bounded. If there exists a common positive definite matrix P and Z_i such that the linear matrix inequalities (11) are feasible, then the estimation error converges to zero exponentially.* ■

We can solve linear matrix inequalities (11) using powerful packages like MATLAB linear matrix inequality Toolbox to obtain P and Z_i where observer gains $L_i = P^{-1} Z_i$.

V. Controller Synthesis By Virtual Desired Variables

Due to the exponential convergence of estimation error, we directly use $\widehat{\lambda}(t)$ and $\widehat{v}_m(t)$ instead of $\lambda(t)$ and $v_m(t)$, respectively, to carry out the following controller design. This treatment can simplify the design procedure. The overall VDV design procedure can be described as Fig. 1

A. Mechanical Loop Control

Denote the speed tracking error as $\tilde{v}_m \equiv v_m - v_d$. The tracking error dynamics can be rewritten as $M\dot{\tilde{v}}_m + (D+k_v)\tilde{v}_m = F - F_d + (F_d - F_l - Dv_d - M\dot{v}_d + k_v\tilde{v}_m)$, where F_d denotes the desired force to produce the desired speed; k_v is an adjustable damping ratio. For speed tracking control, the desired force is selected as $F_d = F_l + Dv_d + M\dot{v}_d - k_v\tilde{v}_m$. This yields the following error dynamics

$$M\dot{\tilde{v}}_m + (D+k_v)\tilde{v}_m = F - F_d \tag{12}$$

If $F - F_d$ is driven to zero, the mover speed will converge to the desired value. Therefore, the speed tracking control problem is reformulated into the force tracking problem. Then the concept of VDVs is introduced in the following to achieve this objective.

B. Electrical Loop Control

The following design scheme is somewhat similar to the well-known backstepping control [16]. However, for our problem, direct implementation of backstepping control not trivial due to the highly coupled nonlinearity of the LIM. Next, we consider the electrical dynamics (2). Let the VDVs consist of the virtual desired current (x_{1d}, x_{2d}) and virtual desired flux (x_{3d}, x_{4d}). Then, the desired current and desired flux are designed such that the electrical subsystem provides the desired force F_d. To this end, the VDVs is specified by satisfying:

- desired force

$$F_d = \kappa\left(x_{2d}x_{3d} - x_{1d}x_{4d}\right) \tag{13}$$

;

- constant desired flux

$$c^2 = x_{3d}^2 + x_{4d}^2. \tag{14}$$

Notice that the condition (14) is to achieve the optimal generated force. Define the error signal for the electrical part as $\underline{\widetilde{x}} = \underline{x} - \underline{x}_d$, where $\underline{\widetilde{x}} = \begin{bmatrix}\tilde{x}_1 & \tilde{x}_2 & \tilde{x}_3 & \tilde{x}_4\end{bmatrix}^\top$ and $\underline{x}_d = \begin{bmatrix}x_{1d} & x_{2d} & x_{3d} & x_{4d}\end{bmatrix}^\top$. The control objective of steering F to track F_d can be achieved if $\underline{\widetilde{x}} \to 0$. To this end, the equation (2) and (12) is rewritten as

$$M\dot{\tilde{v}}_m + (D+k_v)\tilde{v}_m = \varsigma\underline{\widetilde{x}} \tag{15}$$

$$\begin{aligned} &Q\dot{\underline{\widetilde{x}}} + G(v_m)\underline{\widetilde{x}} + R(v_m)\underline{\widetilde{x}} \\ &= \upsilon - \left[Q\dot{\underline{x}}_d + G(v_m)\underline{x}_d + R(v_m)\underline{x}_d\right] \end{aligned} \tag{16}$$

where $\varsigma = \kappa\begin{bmatrix}-x_{4d} & x_{3d} & x_2 & -x_1\end{bmatrix}$. Let $R(v_m) = \bar{R}_1 - \bar{R}_2(v_m)$, where

$$\bar{R}_1 = \begin{bmatrix} \gamma\mathbf{I}_2 + \iota\mathbf{I}_2 & -\frac{R_s}{L_s}\mathbf{I}_2 \\ -\frac{L_mR_s}{L_s}\mathbf{I}_2 & \frac{R_s}{L_s}\mathbf{I}_2 \end{bmatrix},$$
$$\bar{R}_2 = \begin{bmatrix} \iota\mathbf{I}_2 & -\frac{\pi n_p}{\ell}v_m\mathbf{J}_2 \\ 0 & 0 \end{bmatrix}.$$

We will specify the VDVs in Subsection C, such that $\xi_p = \upsilon - \left[Q\dot{\underline{x}}_d + G(v_m)\underline{x}_d + R(v_m)\underline{x}_d\right] + \bar{R}_2(v_m)\underline{\widetilde{x}} + \tilde{v}_m\varsigma^\top$ equals zero, the error system (15) and (16) leads to

$$\begin{bmatrix} M & 0 \\ 0 & Q \end{bmatrix}\begin{bmatrix}\dot{\tilde{v}}_m \\ \dot{\underline{\widetilde{x}}}\end{bmatrix} + \begin{bmatrix} D+k_v & \varsigma \\ \varsigma^\top & G(v_m)+\bar{R}_1 \end{bmatrix}\begin{bmatrix}\tilde{v}_m \\ \underline{\widetilde{x}}\end{bmatrix} = 0$$

Then the stability of the system can be proven by choosing Lyapunov function candidate as $V_c(\underline{\widetilde{x}}(t), \tilde{v}_m) = \frac{1}{2}\underline{\widetilde{x}}(t)^\top Q\underline{\widetilde{x}}(t) + \frac{1}{2}M\tilde{v}_m^2$, which results in $\dot{V}_c(\underline{\widetilde{x}}(t), \tilde{v}_m) = -\underline{\widetilde{x}}^\top\bar{R}_1\underline{\widetilde{x}} - (D+k_v)\tilde{v}_m^2$.It can be checked that the matrix $\bar{R}_1 > 0$ by choosing $\iota > -L_sR_p/L_m$. Hence the exponential stability is shown once the VDVs from $\xi_p = 0$ are well defined.

C. VDV Implementation

In the following, the control law u and VDVs $\underline{x}_d$ are chosen such that $\xi_p = 0$. The condition $\xi_p = 0$ is rewritten as:

$$\begin{aligned} 0 &= \tfrac{L_s}{L_m}u_1 - \sigma\dot{x}_{1d} - \gamma x_{1d} + \tfrac{R_s}{L_s}x_{3d} \\ &\quad + \tfrac{\pi n_p}{\ell}v_m(x_{4d} + \tilde{x}_4) + \iota\tilde{x}_1 - \kappa\tilde{v}_m x_{4d} \end{aligned} \tag{17}$$

$$\begin{aligned} 0 &= \tfrac{L_s}{L_m}u_2 - \sigma\dot{x}_{2d} - \gamma x_{2d} + \tfrac{R_s}{L_s}x_{4d} \\ &\quad - \tfrac{\pi n_p}{\ell}v_m(x_{3d} + \tilde{x}_3) + \iota\tilde{x}_2 + \kappa\tilde{v}_m x_{3d} \end{aligned} \tag{18}$$

$$\dot{x}_{3d} = \tfrac{L_mR_s}{L_s}x_{1d} - \tfrac{\pi n_p}{\ell}v_m x_{4d} - \tfrac{R_s}{L_s}x_{3d} + \kappa\tilde{v}_m x_2 \tag{19}$$

$$\dot{x}_{4d} = \tfrac{L_mR_s}{L_s}x_{2d} + \tfrac{\pi n_p}{\ell}v_m x_{3d} - \tfrac{R_s}{L_s}x_{4d} - \kappa\tilde{v}_m x_1. \tag{20}$$

From the constraint (14), we set

$$\begin{bmatrix}x_{3d} \\ x_{4d}\end{bmatrix} = \begin{bmatrix} c\cos(\rho(t)) \\ c\sin(\rho(t)) \end{bmatrix}, \tag{21}$$

where the variable $\rho(t)$ is determined later. In turn,

$$\begin{bmatrix}\dot{x}_{3d} \\ \dot{x}_{4d}\end{bmatrix} = \dot{\rho}\mathbf{J}_2\begin{bmatrix}x_{3d} \\ x_{4d}\end{bmatrix}. \tag{22}$$

Substituting (22) into (19) and (20), we have

$$\begin{aligned} \begin{bmatrix}x_{1d} \\ x_{2d}\end{bmatrix} &= \tfrac{1}{L_m}\left(\tfrac{L_s}{R_s}\left(\dot{\rho} - \tfrac{\pi n_p}{\ell}v_m\right)\mathbf{J}_2 + \mathbf{I}_2\right)\begin{bmatrix}x_{3d} \\ x_{4d}\end{bmatrix} \\ &\quad + \tfrac{\kappa L_s}{L_mR_s}\tilde{v}_m\mathbf{J}_2\begin{bmatrix}x_1 \\ x_2\end{bmatrix}. \end{aligned} \tag{23}$$

Since the desired states also satisfy (13), substituting (23) into (13) yields

$$\dot{\rho}(t) = \tfrac{\pi n_p}{\ell}v_m + \tfrac{L_mR_s}{\kappa L_s c^2}F_d - \tfrac{\kappa}{c^2}\tilde{v}_m\left(x_1x_{3d} + x_2x_{4d}\right), \tag{24}$$

where $\rho(t)$ is thus defined. Furthermore, to satisfy (17) and (18), the control law is formulated as follows:

$$\begin{aligned} u &= \tfrac{L_m}{L_s}\sigma\begin{bmatrix}\dot{x}_{1d} \\ \dot{x}_{2d}\end{bmatrix} + \tfrac{L_m}{L_s}\gamma\begin{bmatrix}x_{1d} \\ x_{2d}\end{bmatrix} - \tfrac{L_m}{L_s}\iota\begin{bmatrix}\tilde{x}_1 \\ \tilde{x}_2\end{bmatrix} \\ &\quad + \tfrac{\pi n_p L_m}{\ell L_s}v_m\mathbf{J}_2\begin{bmatrix}\tilde{x}_3 \\ \tilde{x}_4\end{bmatrix} \\ &\quad + \left(\left(\tfrac{\pi n_p L_m}{\ell L_s}v_m - \tfrac{L_m\kappa}{L_s}\tilde{v}_m\right)\mathbf{J}_2 - \tfrac{L_mR_s}{L_s^2}\mathbf{I}_2\right)\begin{bmatrix}x_{3d} \\ x_{4d}\end{bmatrix} \end{aligned} \tag{25}$$

The implementation of the control law (25) is complicated due to the first term on the right-hand side, which includes the time derivative of x_{1d} and x_{2d}. Fortunately,

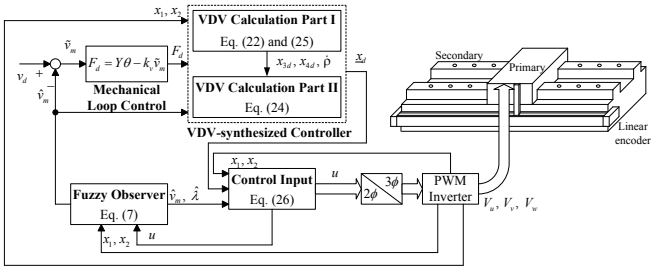

Fig. 2: The structure of the VDV-synthesis controller.

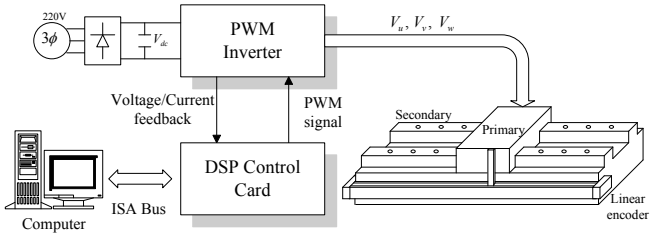

Fig. 3: The experimental setup.

the exponential stability shown in Subsection B make the controller very robust to uncertainty. This feature allows the approximation $\dot{x}_{id} \approx x_{id} - \overline{x}_{id}$, where $\dot{\overline{x}}_{id} + \overline{x}_{id} = x_{id}$. The simplified control law will be adopted in our experiment. The overall structure of the control law with control parameters is illustrated in Fig. 2.

VI. Experimental Results

To further verify the validity of the proposed scheme, several experiments of sensorless speed control are described in this section. The experimental setup is shown in Fig. 3. In our experiments, the developed controller is realized by a DSP-based control card (Simu-Drive system), which takes the TMS320F2812 DSP (fixed-point 32-bit) as the main control core. The DSP control card also provides multichannel of A/D and encoder interface circuits. Here, three-phase voltages and currents are sampled by the A/D converters and fed into the DSP-based controller. The speed is measured by a linear encoder with precision 20μm for one pulse. In addition, the block-building MATLAB Simulink Toolbox and Real-Time Workshop are taken as an interface between software and hardware. When the build-up controller block is established, the Real-Time Workshop plays a role of a compiler to transform the controller into a C code, which is download to the DSP-based control card. The specifications and parameters of the LIM are listed in Table I.

TABLE I

The Specification And Parameters Of The Linear Induction Motor

Rated Specification		Parameters	
Pole Pair	2	R_p	13.2 Ω
Power	1 HP	R_s	11.78 Ω
Voltage	240 V	L_p	0.42 H
Current	5 A	L_s	0.42 H
Pole pitch	$0.0465\ m$	L_m	0.4 H
Secondary length	$0.82\ m$	M	$4.775\ kg$
		D	$53\ kg/s$

The speed control parameters are chosen as follows: $k_v = 1000$, $c = 0.55$, and $\iota = 0.1$. The immeasurable premise variables $\hat{\lambda}_{sa} \in \begin{bmatrix} D_1 & d_1 \end{bmatrix} = \begin{bmatrix} 0.8 & -0.8 \end{bmatrix}$, $\hat{\lambda}_{sb} \in \begin{bmatrix} D_2 & d_3 \end{bmatrix} = \begin{bmatrix} 0.8 & -0.8 \end{bmatrix}$, and $\hat{v}_m \in \begin{bmatrix} D_3 & d_3 \end{bmatrix} = \begin{bmatrix} 4 & -4 \end{bmatrix}$. According to the linear matrix inequality (11), we let $U = diag\{0.9,\ 0.5,\ 0.5,\ 0.4,\ 2.81\}$ and $E = diag\{12,\ 1.9,\ 7,\ 7.3,\ 1.9\}$, then the observer gains are obtained by solving LMI toolbox of MATLAB are given below:

$$L_i = \begin{bmatrix} -524.9 & l_{i1} \\ l_{i2} & -599.4 \\ 217.9 & l_{i3} \\ l_{i4} & 217.9 \\ l_{i5} & l_{i6} \end{bmatrix},$$

where the entries $l_i = (l_{i1},\ l_{i2},\ l_{i3},\ l_{i4},\ l_{i5},\ l_{i6})$ are given in following:

$$\begin{aligned}
l_1 &= (-358.2,\ 358.2,\ -0.05,\ -0.002,\ 968.2,\ -968.2) \\
l_2 &= (195.9,\ -195.9,\ 0.05,\ 0.007,\ 968.2,\ -968.2) \\
l_3 &= (401.2,\ -401.2,\ -0.05,\ -0.02,\ -968.2,\ -968.2) \\
l_4 &= (735.8,\ -735.8,\ 0.04,\ -0.01,\ -968.2,\ -968.2) \\
l_5 &= (-126.7,\ 126.7,\ -0.05,\ -0.009,\ 968.2,968.2) \\
l_6 &= (60.1,\ -60.1,\ 0.05,\ 0.01,\ 968.2,\ 968.2) \\
l_7 &= (494.1,\ -494.1,\ -0.05,\ -0.03,\ -968.2,\ 968.2) \\
l_8 &= (-133.8,\ 133.8,\ 0.05,\ 0.01,\ -968.2,\ 968.2)\,.
\end{aligned}$$

Based on this setting, the following speed control experiments are performed.

Experiment *Sinusoidal Speed Tracking*

Consider the speed tacking for the sinusoidal $v_d = 0.5 \sin \pi t\ m/\sec$. The desired and actual speed, actual and estimated speed are shown in Figs. 4(a) and 4(b), respectively. The speed estimation error is shown in Fig. 4(c). The primary voltage of u-phase V_u and primary current of u-phase i_u are shown in Figs. 5(a) and 5(b), respectively. Furthermore, the desired and estimation secondary flux of one phase are shown in Fig. 5(c).

In order to investigate the robustness of the proposed control scheme, the primary and secondary resistance variations are considered here, i.e., assuming the actual $\overline{R}_s$ and $\overline{R}_p$ to be $R_s * 1.2$ and $R_p * 1.4$, respectively. Then, experimental results for the desired and actual speed, actual and estimated speed, speed estimation error are shown in Figs. 6(a), 6(b), and 6(c), respectively. The primary voltage of u-phase V_u and primary current of u-phase i_u are shown in Figs. 7(a) and 7(b), respectively. As we can see, the fuzzy observer performs well even with uncertainties in the system.

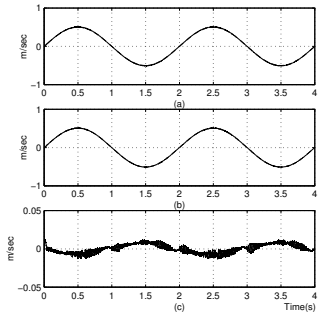

Fig. 4: Sinusoidal speed tracking, (a) desired speed (−−) and actual speed (—), (b) estimated speed (−−) and actual speed (—), (c) speed estimation error.

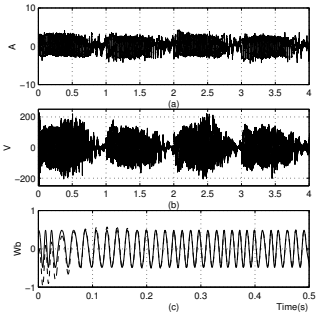

Fig. 5: Sinusoidal speed tracking, (a) primary current for one phase, (b) primary voltage for one phase (c) estimated (−−) and desired (—) secondary fluxes λ_{sa}.

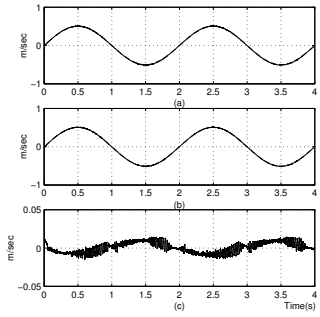

Fig. 6: Sinusoidal speed tracking with parameter uncertainty, (a) desired speed (−−) and actual speed (—), (b) estimated speed (−−) and actual speed (—), (c) speed estimation error.

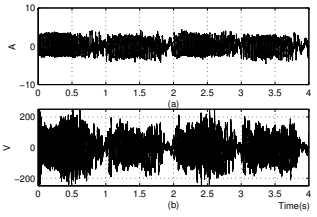

Fig. 7: Sinusoidal speed tracking with parameter uncertainty, (a) primary current for one phase, (b) primary voltage for one phase.

VII. Conclusions

This paper has presented a sensorless speed control scheme of LIMs based on the T-S fuzzy observer. The T-S fuzzy observer algorithm has been used to estimation the mover speed and secondary flux of the LIM, where the observer gains are obtained by solving a set of linear matrix inequalities. The two-stage design technique and the synthesis of using virtual desired variables are applied to construct the controller for the speed tracking purpose. The experimental results have shown the good transient responses and zero speed tracking errors in the steady state. One more thing that deserves to be mentioned is that the stability discussed in this paper is exponentially stable. This means that the proposed control method is very robust and tolerates system uncertainty.

References

[1] I. Takahashi and Y. Ide, "Decoupling control of thrust and attractive force of a LIM using a space vector control inverter," *IEEE Trans. Ind. Appl.*, vol. 29, no. 1, pp. 161-167, Jan./Feb. 1993.

[2] Z. Zhang, T. R. Eastham, and G. E. Dawson, "Peak thrust operation of linear induction machines from parameter identification," *IEEE Industry Applications Thirtieth IAS Annual Meeting,* Orlando, Florida USA, Oct. 1995, pp. 375-379.

[3] G. H. Abdou and S. A. Sherif, "Theoretical and experimental design of LIM in automated manufacturing systems," *IEEE Trans. Ind. Appl.*, vol. 27, no. 2, pp. 286-293, Mar./Apr. 1991.

[4] C. I. Huang and L. C. Fu, "Adaptive approach to motion controller of linear induction motor with friction compensation," *IEEE/ASME Trans. Mechatronics*, vol. 12, no. 4, pp. 480-490, Aug. 2007.

[5] V. H. Benitez, A. G. Loukianov, and E. N. Sanchez, "Neural identification and control of a linear induction motor using an $\alpha - \beta$ model," *in Proc. American Control Conf.*, Denver, Colorado, June 2003, pp. 4041-4046.

[6] H. Amirkhani and A. Shoulaie, "Online control of thrust and flux in linear induction motors," *Proc. Inst. Electr. Eng.-Electr. Power Appl.*, vol. 150, no. 5, pp. 515-520, Sept. 2003.

[7] H. M. Ryu, J. I. Ha, and S. K. Sul, "A new sensorless thrust control of linear induction motor," *IEEE Industry Applications Thirty-Fifth IAS Annual Meeting*, Roma, Italy, Oct. 2000, pp. 1655-1661.

[8] T. Takagi and M. Sugeno, "Fuzzy identification of systems and its applications to modeling and control," *IEEE Trans. Syst., Man, Cybern.*, vol. SMC-15, no.1, pp. 116-132, Jan. 1985.

[9] K. Y. Lian, C. Y. Hung, C. S. Chiu, and P. Liu, "Induction motor control with friction compensation: An approach of virtual-desired-variable synthesis," *IEEE Trans. Power Electronics*, vol. 20, no. 5, pp. 1066-1074, Sep. 2005.

[10] I. Boldea and S. A. Nasar, *Linear Electric Actuators and Generators*. Cambridge, U.K.: Cambridge Univ. Press, 1997.

[11] S. A. Nasar and I. Boldea, *Linear Motion Electric Machines*. John Wiley & Sons, Inc., 1976.

[12] B. K. Bose, *Power Electronics and Motor Drives: Advances and Trends.* Academic Press, 2006.

[13] E. F. da Silva, C. C. dos Santos, and J. W. L. Nerys, "Field oriented control of linear induction motor taking into account end-effects," *in Proc. AMC*, Kawasaki, Japan, March 2004, pp. 689-694.

[14] J. H. Sung and K. Nam, "A new approach to vector control for a linear induction motor considering end effects," *IEEE Industry Applications Thirty-Fourth IAS Annual Meeting*, Phoenix, Arizona USA, Oct. 1999, pp. 2284-2289.

[15] K. Y. Lian and C. Y. Hung, "Sensorless control for induction motors via fuzzy observer design," *in Proc. ISIE*, Montréal, Canada, July 2006, pp. 2140-2145.

[16] M. Krstić, I. Kanellakopoulos, P. Kokotović, *Nonlinear and Adaptive Control Design*. New York, John Wiley & Sons, 1995.